Electrochemical and Solid-State Letters, **9** (4) C77-C80 (2006)
1099-0062/2006/9(4)/C77/4/$20.00 © The Electrochemical Society

Study on Mechanically Induced Current Suppression and Super Filling Mechanisms

Bülent M. Başol[a,*,z] and Alan C. West[b,*]

[a]*ASM NuTool, Incorporated, Fremont, California 94538, USA*
[b]*Department of Chemical Engineering, Columbia University, New York, New York 10027, USA*

Electrochemical mechanical deposition of copper on a patterned wafer surface involves sweeping the surface with a pad during deposition and yields a planarized copper layer. In this work, the mechanism of this planarization phenomenon was studied by electroplating copper films on blanket wafer surfaces while sweeping a portion of the wafer surface with a small pad. Suppression of current density within the swept region was observed in the case when both organic suppressor and accelerator additives were present in the plating electrolyte. The degree of suppression in the deposition current density was found to be a strong function of the wafer rotation speed. Experimental and modeling results agreed well with the mechanically induced super filling mechanism which suggests that the difference between the current densities at the swept and unswept regions on the wafer surface is due to an additive surface coverage differential created by the sweeping action of the pad.
© 2006 The Electrochemical Society. [DOI: 10.1149/1.2173191] All rights reserved.

Manuscript submitted November 11, 2005; revised manuscript received December 22, 2005.
Available electronically February 14, 2006.

Electrochemically deposited (ECD) copper is the preferred material for the fabrication of advanced interconnect structures for integrated circuits.[1] In an interconnect fabrication process, copper is filled into and coated over the various size features, such as trenches and vias, formed in the dielectric layers on wafer surfaces. In a typical ECD process, specially formulated electrolytes containing chloride ions and organic additives such as suppressors and accelerators, are employed to achieve void-free super-filling or bottom-up filling of submicrometer size high aspect-ratio (AR) features.[2-4] This super-filling mechanism is not operative in the large features with aspect ratios much smaller than 1. The surface topography of a copper layer deposited on a patterned wafer surface by the ECD process, therefore, is nonplanar since ECD coats the low AR features in a conformal manner so that steps form at the edges of such large features. In the standard copper interconnect fabrication process the plated copper is annealed and its portion over the top surface or the field region is first planarized and then removed by chemical mechanical polishing (CMP), electrochemical mechanical polishing (ECMP), or by a combination of both approaches leaving the metal only within the cavities of the features.

The electrochemical mechanical deposition (ECMD) process was developed to planarize the copper layer during its deposition step so that an already planarized film would be delivered to the CMP process.[5,6] The benefits of such planar copper layers for interconnect fabrication have already been discussed and demonstrated.[7-9] Since the well-known super fill mechanisms for the high AR features do not apply to filling low AR features, ECMD utilizes a newly identified mechanically induced super-filling (MISP) mechanism to achieve planarization of copper over large features on patterned wafer surfaces.

ECMD, as applied to copper deposition on patterned wafers, involves sweeping the surface of the wafer with pad strips as electroplating commences. When this mechanical action is applied to the wafer surface during plating, the process provides enhanced deposition of copper into the large features which may even have aspect-ratios of smaller than 0.01.[6,7,10] The MISP mechanism was recently studied and a model was proposed.[10] According to this model, the sweeping action of the planarization pad induces a differential in the copper growth rates between the top surface of the wafer and the cavities by changing the surface coverage of active organic additives at the top surface. Accordingly, every time the planarization pad strip sweeps a region on the top surface of the wafer, it lowers the effective surface coverage of accelerators at that location and increases the suppressor coverage. Since sweeping does not directly affect the cavities, the surface coverage of accelerator and suppressor within the cavities is undisturbed. Therefore, during plating less current density goes to the top surface due to higher suppression compared to the cavities which have higher fractional accelerator surface coverage. In this respect MISP is a result of a mechanically induced current suppression (MICS) mechanism which occurs at the mechanically swept portion, i.e., the top surface, of the substrate.

If the above hypothesis is correct, then a differential could be induced between the growth rate of Cu at a swept and an unswept region of a flat surface when a small pad is used to sweep only a part of the surface in a plating electrolyte containing accelerator and suppressor species. In this study we developed an experimental approach to study MICS by partially sweeping unpatterned blanket wafer surfaces during copper deposition.

Experimental

A schematic top view of the plating cell used in the experiments is shown in Fig. 1. The shaping plate is a porous rigid plate through which the plating solution rises up and reaches the wafer surface to be plated. The porosity on the shaping plate was designed to shape the electric field and thus assure uniform film deposition. A rectangular copper anode was placed in a cavity under the shaping plate and a small (8×20 mm) piece of a planarization pad was attached over the shaping plate. The planarization pad was a fixed-abrasive type material supplied by 3M Company, and it had a soft subpad made of a spongy material. The wafer was lowered face-down toward the shaping plate with a holder that could rotate as well as translate in the x direction by controlled amounts and at controlled speeds. Multiple electrical contacts were made to the wafer surface at the two locations indicated in Fig. 1. When the wafer was lowered down toward the shaping plate, the wafer surface touched the plating solution while being pushed against the surface of the pad pieces at a preselected force level of about 0.8 psi. Blanket wafers of 200 mm diameter were used in this study. Substrates were sputter-coated with a 40 nm thick Ta barrier layer and a 100–120 nm thick copper seed before plating. A high acid Cu-sulfate electrolyte with 17 g/L of Cu, 175 g/L of H_2SO_4, and 50 ppm of Cl^- was used for plating. Cubath Viaform suppressor and accelerator available from Enthone were used as the organic additives. Depositions were carried out on blanket wafers out of electrolytes with different additive contents while touching the surface of the wafer with the pad piece. Rotation of the wafer and physical contact with the pad piece generated a swept ring on the wafer surface during the plating process between radial positions of 55 and 75 mm from the center. The swept ring is shown as the shaded area in the top view of Fig. 1. Right after deposition, Cu thickness profiles were measured along the wafer radius across the swept ring. This way differences between deposition current density at the swept ring and the unswept region

* Electrochemical Society Active Member.
z E-mail: bulent.basol@asm.com

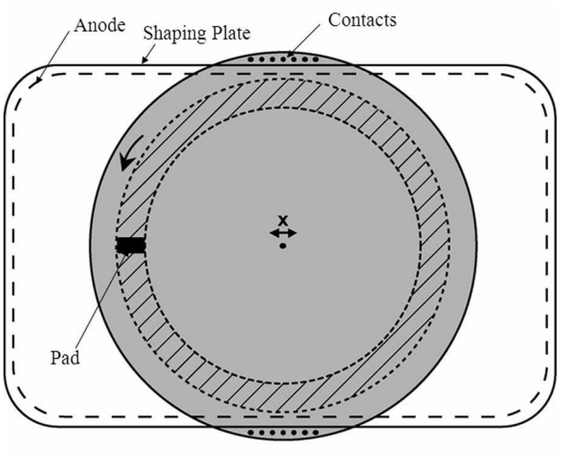

Figure 1. Top view of the plating cell employed in the experiments.

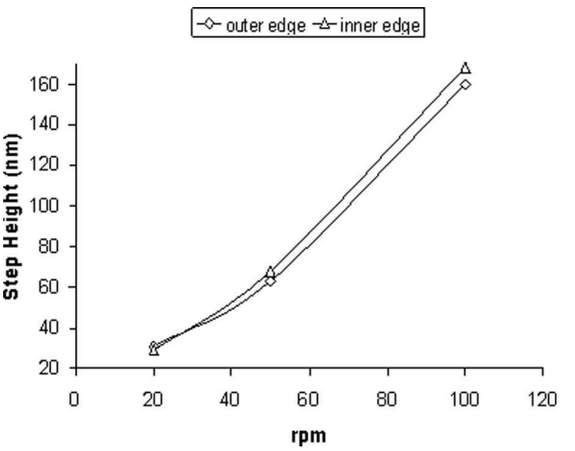

Figure 3. Step heights measured at the outer and inner edge of the swept portion as a function of rpm. A solution with $A = 2$, $S = 8$ was used in the experiment.

could be studied as a function of the electrolyte composition and wafer rotation speed. The plating cell was carefully cleaned and the copper anode was etched after each plating experiment and before introducing the next electrolyte. This was found to be very important to avoid cross contamination of experimental baths by the organic additives. Wafers were translated by ±1 mm in the *x*-direction at a speed of 5 mm/s during processing to improve uniformity of pad sweeping. A four-point probe was used to measure the copper layer thicknesses, which were also confirmed by focused ion beam (FIB) cross sections to avoid any possible error due to copper resistivity differences between the swept and unswept regions. Such resistivity differences are not expected based on our previously published data,[11] and none was observed in the present experiments.

Results

Figure 2 shows a set of thickness profiles taken across the swept region of four blanket wafers plated in four different electrolytes using a single pad piece and a rotation speed of 100 rpm. The current density was 20 mA/cm^2 during plating and about 5500 Å of copper was deposited on the wafers based on the plating charge applied. As can be seen from this data the Cu thickness profile taken across a 40 mm wide segment of the wafer radius was relatively uniform for wafers processed in additive-free VMS ($A = 0$ mL/L, $S = 0$ mL/L) and the solution containing only accelerators, A ($A = 2$ mL/L, $S = 0$ mL/L), suggesting no or little influence on the plating current density by the sweeping pad. For the electrolyte containing only suppressors, S ($A = 0$ mL/L, $S = 8$ mL/L) there is a small step of about 500 Å at the interface of the swept and unwept regions. On the contrary, the Cu thickness was significantly lower

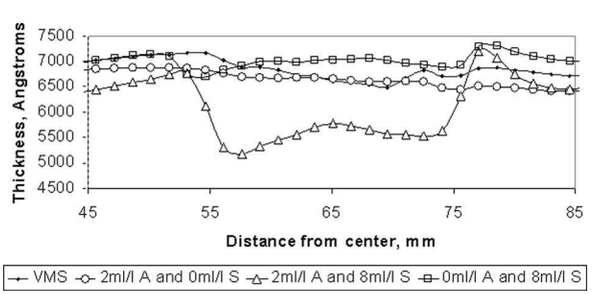

Figure 2. Cu thickness profiles taken across the swept portion of blanket wafers plated in electrolytes with various accelerator (A) and suppressor (S) concentrations (in units of mL/L). The swept portion lies within a ring with outer and inner radii of 75 and 55 mm, respectively.

within the swept ring of the wafer plated in the electrolyte containing both the suppressor and the accelerator species ($A = 2$ mL/L, $S = 8$ mL/L). The step height between the unswept and swept regions of the wafer surface is about 1600 Å for this sample demonstrating that sweeping by the pad piece caused about 30% reduction in the copper growth rate within the swept ring. The pad piece is expected to shadow some of the deposition current in the swept ring since it is insulating and does not allow deposition on the surface segment it is covering at any instant during plating. This shadowing effect can be easily calculated.

Since the inner and outer diameters of the swept ring are 75 and 55 mm, respectively, the area of the swept ring is $3.1416 \times (7.5^2 - 5.5^2) = 81.68$ cm^2. The area of the pad piece, on the other hand, is only 1.6 cm^2. Therefore, the shadowing effect due to the pad piece would be about 1.6/81.68 = 1.9%, and it would not be a function of rpm. Obviously, the 1.9% shadowing effect cannot explain the experimentally found 30% reduction in the copper deposition rate in the swept region. Furthermore, the shadowing effect would be the same for all wafers irrespective of the plating chemistry used. The results, however, pointed to the fact that only the chemistry containing both suppressor and accelerator species showed the large reduction in the deposition rate onto the swept ring portion of the wafer and that the step height was a strong function of rpm.

Figure 3 shows the dependence of the step heights measured at the outer and inner edges of the swept ring as a function of rpm for wafers plated in an electrolyte with $A = 2$ mL/L and $S = 8$ mL/L. Data in both Fig. 2 and Fig. 3 are in qualitative agreement with the previously reported MISF mechanism of ECMD,[10] wherein pad sweeping decreases accelerator effectiveness and increases suppressor effectiveness at the swept area, and the time period between pad sweeps, i.e., the rpm, determines the magnitude of the Cu thickness differential between the swept and unswept regions. As the time period between sweeps gets smaller (higher rpm), the thickness difference gets larger because the accelerator is not allowed to fully readsorb on the swept surface replacing already adsorbed suppressor.

Modeling

The problem in hand was modeled by assuming a 2 cm long swept surface area of the blanket wafer in the plating solution. It was assumed that the current and thickness distributions are governed by Laplace's equation for the electrical potential

$$\nabla^2\phi = 0 \quad [1]$$

where the counter electrode (anode) is placed parallel to the wafer at a distance of 15 mm. The exact position of the anode is not important for distances larger than roughly 10 mm. Along the wafer surface, we assume modified Tafel kinetics

$$-\kappa\frac{\partial\phi}{\partial z} = i = i_o(1-\theta_{no,pad})\exp\left(\frac{-\alpha_c F}{RT}(V-\phi_o)\right) \quad [2]$$

in the regions where the pad sweeping is not present, and

$$-\kappa\frac{\partial\phi}{\partial z} = i = i_o[1-\theta_{no,pad}-\theta_{pad,o}\exp(-kt)]\exp\left[\frac{-\alpha_c F}{RT}(V-\phi_o)\right] \quad [3]$$

in regions where the pad piece sweeps over the surface. Because of the additive relaxation kinetics implicit in Eq. 3, the current distributions were calculated at discrete times, approximately 20 time steps per revolution of a wafer. The shadowing effect was ignored. Implicit in the numerical approach is the assumption of a periodic behavior due to the pad motion. In other words, it is assumed that the pad completely restores the surface to the same condition after each sweep. After a sufficiently long time, a periodic behavior may be expected. In our experiments the plating time was slightly over 1 min and the number of pad-passes varied between 20 and over 100. Nevertheless, experimental validation of when exactly the periodic behavior is reached could not be done in this set of experiments.

The time-average current distribution at each radial position on the wafer was calculated, and the final variation in simulated thickness distribution was estimated from

$$\lambda(r) = \lambda_{seed} + \lambda_{avg,plate}\frac{\bar{i}(r)}{i_{avg}} \quad [4]$$

where the normalized time-average current distribution is given by

$$\frac{\bar{i}(r)}{i_{avg}} = \frac{\int_0^{1/\Omega} i(r)dt}{\frac{2}{r_o^2}\int_0^{r_o}\left(\int_0^{1/\Omega} i(r)dt\right)rdr} \quad [5]$$

The thickness distribution resulting from these simulations depends on four groups of parameters

$$Wa_T = \frac{RT\kappa}{\alpha_c F i_{avg} w_{pad}}, \quad \theta_o = \frac{\theta_{pad,o}}{1-\theta_{no,pad}}, \quad r_o/w_{pad}, \quad \text{and } k/\Omega \quad [6]$$

For simulations corresponding to the experimental conditions presented here, $Wa_T = 0.51$ and $r_o/w_{pad} = 5$. Furthermore, it is assumed that $\lambda_{seed} = 110$ nm and $\lambda_{plate,avg} = 550$ nm. Furthermore, as described below, the value of k can be estimated from previous work.

In Ref. 10, a relationship was derived between the planarization factor, n, and the additive relaxation rate constant k, where n was defined as the ratio of the copper thickness deposited within the wafer cavities to the copper thickness deposited on the top surface which was swept by the pad

$$n = [i_{avg}t_p - (1-D)(i_{h0}-i_{avg})(1-e^{-ktp})/kD]/[i_{avg}t_p + (i_{h0}-i_{avg}) \times (1-e^{-ktp})/k] \quad [7]$$

In the experiments of Ref. 10 pattern wafers were subjected to an ECD-ECMD process flow. In other words the surface of the patterned wafer was first plated with a thin copper layer in the ECD mode in an electrolyte containing accelerator and suppressor species. Then ECMD was initiated by pressing the pad on the wafer surface. The best fit of Eq. 7 to the measured data in Ref. 10 was found for $D = 0.2$, $i_{h0} = 0.01$ A/cm^2, and $i_{l0} = 0.06$ A/cm^2, where

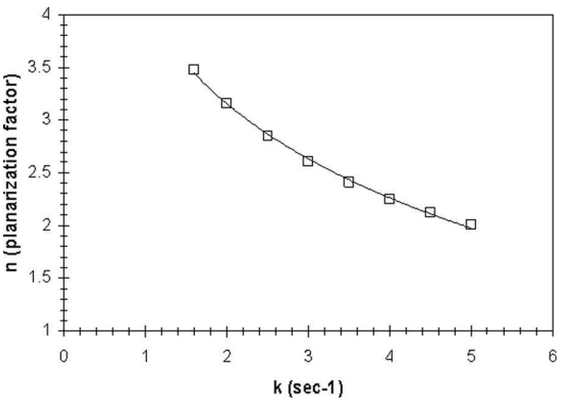

Figure 4. Expected variation of planarization factor, n, with the additive relaxation rate constant, k. Point at $n = 3.5$, $k = 1.6$ s^{-1} was experimentally determined in Ref. 10 for the ECMD process performed on a patterned wafer in high acid copper plating electrolyte with $A = 2$, $S = 8$ using a single pad strip along the wafer diameter. Wafer rotation was 50 rpm, and data was collected from features located 80 mm from the wafer center.

D is the wafer pattern density and i_{h0} and i_{l0} are the current densities right after pad sweeping at the top surface and within the cavities of the wafer, respectively. The average current density, i_{avg}, was 20 mA/cm^2 and the electrolyte was similar to the one used in the present work, i.e., a high acid electrolyte with 2 mL/L accelerator and 8 mL/L suppressor. We plotted the planarization factor n as a function of k in Fig. 4 for a wafer rpm of 50, which corresponds to a plating time between pad sweeps of $t_p = 0.557$ s at locations 20 mm away from the edge of the wafer. The planarization factor value of about 3.5 found in Ref. 10 for the experimental conditions reviewed above indicates a value of about 1.6 (s)$^{-1}$ for k.

In a more recent study, we investigated the dependence of planarization efficiency in the ECMD process on various process parameters.[12] In those experiments the ECMD process was directly carried out on the seed layers of patterned wafers without the initial ECD step of Ref. 10 and lower planarization factors of about 2 were obtained near the edge of the wafers in high acid electrolyte compositions similar to those in Ref. 10 and the present work. A planarization factor of two corresponds to a k value of about five according to the relationship shown in Fig. 4. With an uncertainty in the pattern density which may vary between 20 and 30%, the k value may also vary between about four and five. These experimental findings suggest that additive adsorption kinetics on virgin copper seed layers are different than additive adsorption kinetics on electroplated copper surfaces which are previously exposed to electrolytes with organic additives. The impact of derivatization of substrate surfaces on planarization efficiency of the ECMD process is presently under study and will be the subject of a future publication.

Since experiments in the present work were carried out by initiating plating and pad sweeping directly on the seed layers of the blanket wafers, the k values to interpret the data need to be selected accordingly. The plot in Fig. 4 is for a wafer rotating at 50 rpm with the wafer surface being swept by a long pad strip extending along the full diameter of the wafer which was the experimental setup used in Ref. 10 and 12. In the present work, on the other hand, only one pad piece is utilized for sweeping the surface. Therefore, the plating time between sweeps, t_p, in the present experimental setup is double that of the experimental setup of Ref. 10 and 12 for a given rpm. In other words, the data shown in Fig. 4 may be used in interpreting the present results for the case of wafers processed at a rotation speed of 100 rpm.

Using $k = 5$ s^{-1}, the last parameter θ_o was fit to experimental results obtained at $\Omega = 100$ rpm, and a reasonable agreement with experiment was found for the other experimental results at 20 and 50 rpm as shown in Fig. 5. Experimental points in Fig. 5 are the

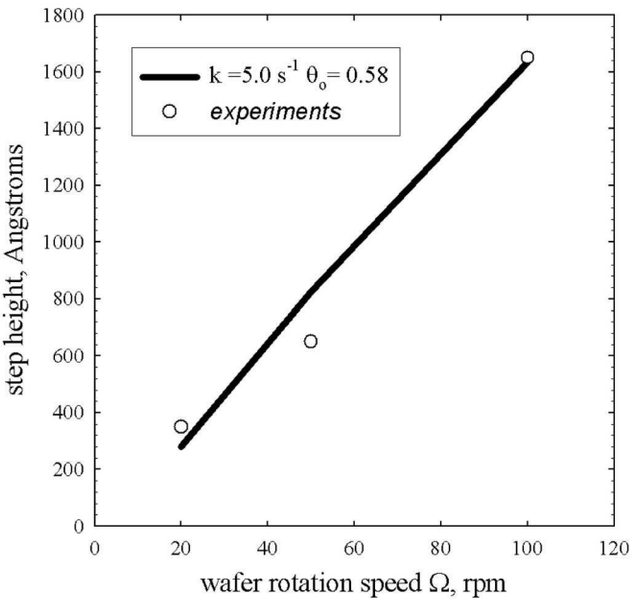

Figure 5. Model-predicted and experimentally determined dependence of step height at the swept/unswept surface interface as a function of wafer rotation rate. A solution with $A = 2$, $S = 8$ was used in the experiment.

average values of step heights measured at the outer and inner edges of the pad piece and plotted in Fig. 3. Figure 6 shows the model predicted thickness distribution (for $k = 5.0\ s^{-1}$, $\theta_o = 0.58$) across the swept ring for various rotation speeds Ω. The modeling result agrees well with the experimental result for $\Omega = 100$ rpm shown in Fig. 2 (in the presence of suppressor and accelerator). They also capture the thickness variation trends shown in Fig. 2, such as the thickness profile peaking at the swept/unswept region of the interface and the bowing of the thickness profile within the swept ring.

Conclusions

The mechanically induced current suppression mechanism was studied by sweeping a portion of a blanket wafer surface by a small pad during copper electroplating, and investigating the effects of sweeping speed and electrolyte composition on the copper growth rate at the swept and unswept regions. Results confirmed that pad sweeping of the wafer surface during plating in an electrolyte containing both suppressor and accelerator species causes an increase in suppressor-to-accelerator surface coverage ratio at the swept region. The accelerator then readsorbs on the swept surface replacing the suppressor at a rate determined by a relaxation rate constant, the magnitude of which depends on the nature of the copper surface. Modeling predictions of the copper thickness profile through the swept portion of the wafer surface and the rpm dependence of the thickness differential between the swept and unswept regions agreed well with the experimental data. These results confirm the previously postulated mechanism for mechanically induced super filling phenomenon that results in planarization of copper layers deposited on patterned wafers by the electrochemical mechanical deposition technique.

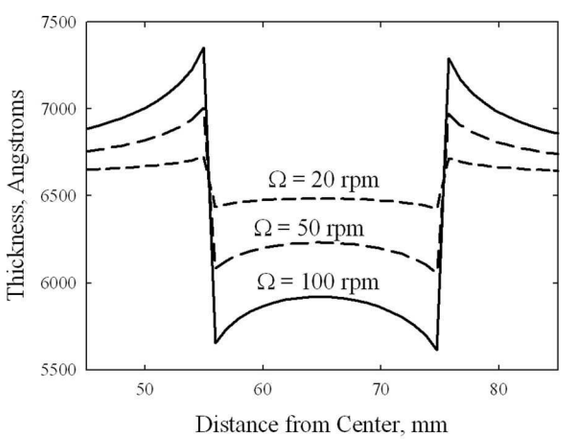

Figure 6. Model-predicted copper thickness profiles across the swept ring on the blanket wafer surface as a function of the wafer rotation rate.

Acknowledgments

B.M.B. acknowledges contributions of his colleagues Tony Wang and Ayse Durmus for carrying out experiments, data collection, and discussions.

ASM NuTool Incorporated assisted in meeting the publication costs of this article.

List of Symbols

F	Faraday's constant, 96,487 C/mol
i	current density, a function of position and time, mA cm^{-2}
$\bar{i}$	time-average current density, a function of position, mA cm^{-2}
i_{avg}	average current density, assumed to be 20 mA cm^{-2}
k	additive relaxation rate constant, s^{-1}
r_o	wafer radius, 10 cm
R	8.314 J mol K^{-1}, the gas constant
T	absolute temperature, 298 K
Wa_T	Tafel Wagner number, defined by Eq. 6
w_{pad}	pad length or the width of swept region, 2 cm

Greek

α_c	transfer coefficient, assumed to be 0.5
λ_{seed}	seed layer thickness, assumed to be 110 nm
$\lambda_{plate,avg}$	average plated film thickness, assumed to be 550 nm.
κ	electrolyte conductivity, assumed to be 0.4 Ω^{-1} cm^{-1}
$\theta_{no,pad}$	effective additive coverage without the pad
$\theta_{pad,o}$	initial reduction due to pad in effective additive coverage
θ_o	ratio of effective additive coverages, defined by Eq. 6
Ω	wafer rotation speed, rpm (in graphs) or revolutions per second (in equations)

References

1. P. C. Andricacos, C. Uzoh, J. O. Ducovic, J. Horkans, and H. Deligianni, *IBM J. Res. Dev.*, **42**, 567 (1998).
2. J. Reid and S. Mayer, in *Proceedings of the Advanced Metallization Conference 1999*, p. 53, Materials Research Society, Warrendale, PA (2000).
3. T. P. Moffat, D. Wheeler, W. H. Huber, and J. Josell, *Electrochem. Solid-State Lett.*, **4**, C26 (2001).
4. A. C. West, S. Mayer, and J. Reid, *Electrochem. Solid-State Lett.*, **4**, C50 (2001).
5. H. Talieh, U.S. Pat. 6,176,992 (2001).
6. B. M. Basol, U.S. Pat. 6,534,116 (2003).
7. B. M. Basol, C. Uzoh, H. Talieh, D. Young, P. Lindquist, T. Wang, and M. Cornejo, *Microelectron. Eng.*, **64**, 43 (2002).
8. B. Stickney, B. Nguyen, B. Basol, C. Uzoh, and H. Talieh, *Solid State Technol.*, **46**, 49 (2003).
9. T. Mourier, K. Haxaire, M. Cordeau, P. Chausse, S. DaSilva, and J. Torres, in *Proceedings of the Advanced Metallization Conference 2004*, p. 597, Materials Research Society, Warrendale, PA (2005).
10. B. M. Basol, *J. Electrochem. Soc.*, **151**, C765 (2004).
11. T. Wang, P. Lindquist, S. Erdemli, E. Basol, R. Zhang, C. Uzoh, and B. Basol, *Thin Solid Films*, **478**, 345 (2005).
12. B. M. Basol, S. Erdemli, C. Uzoh, and T. Wang, *J. Electrochem. Soc.*, **153**, C176 (2006).